行政院國家科學委員會專題研究計畫　成果報告

電注入連續性操作光子晶體雷射的製程開發與特性的設計和量測(2/2)

計畫類別：個別型計畫
計畫編號：NSC94-2215-E-009-016-
執行期間：94 年 08 月 01 日至 95 年 07 月 31 日
執行單位：國立交通大學光電工程學系(所)

計畫主持人：李柏璁

計畫參與人員：盧贊文，蔡豐懋

報告類型：完整報告
報告附件：出席國際會議研究心得報告及發表論文
處理方式：本計畫可公開查詢

中　華　民　國 95 年 10 月 31 日

摘要：

在這份報告中，我們呈現從 2005 年 8 月到 2006 年 7 月的研究成果。我們主要著重於準光子晶體雷射共振腔的研究。由於該元件主要的共振模態為具高 Q 值之 WGM，且其模態分佈具中心場量等於零的特性，較一般光子晶體共振腔所具的共振模態更適合類似微型碟狀雷射所採用的電激發結構。首先我們利用有限時域差分法模擬包括八對稱以及十二對稱準光子晶體共振腔的共振模態，並得到了具有強力侷限的 WGM。我們依據模擬結果，藉由我們發展良好的製程技術製作實際元件。我們量測並得到不同元件的雷射特性，並與傳統光子晶體共振腔做比較。同時，我們也成為世界上首次觀察到八對稱準光子晶體共振腔的雷射的研究團隊。此外，我們更針對這兩種不同晶格的共振腔 WGM 模態所造成的元件特性做深入探討。其中我們所發表的包括了極小的元件尺寸(3.5 微米乘 3.5 微米)，極大的製程容忍度（大於 5%)，以及超高的邊模抑制比（大於 30dB）等。

關鍵詞：準光子晶體，半導體雷射，共振腔

Abstract：

The research progress during the project period from August, 2005 to July, 2006 on quasi-periodic photonic crystal laser cavities is presented in this report. The high quality (Q) factor of whispering-gallery-mode (WGM) in quasi-periodic photonic crystal micro-cavity is designed and obtained. Due to its central zero field distribution, comparing with other defect modes in photonic crystal micro-cavity lasers, it is much proper for electrically driven structure used in micro-disk lasers. At first, we calculate the defect mode frequency and mode profile of different cavity geometry in dodecagonal (12-fold) and octagonal (8-fold) quasi-periodic photonic crystal (QPC) micro-cavity by using finite-difference time-domain (FDTD) method. The well-confined WGM is obtained. The real devices are fabricated by our well-developed fabrication technology. We measure and analyze lasing characteristics of these devices and compare them with photonic crystal micro-cavity. In addition, we are the first research group observing the lasing action from octagonal quasi-periodic photonic crystal micro-cavity in the world. Besides, we also investigate on several potential characteristics of 12- and 8-fold QPC micro-cavity with WGM, including ultra-condensed device size (3.5 μm$\times$3.5 μm), large fabrication tolerance (> 5%), laser device with very high side-mode suppression-ratio (SMSR) (> 30dB) and so on. As an active device, these are very potential characteristics in future photonic integrated circuit.

Keywords：Quasi-Periodic Photonic Crystals, Semiconductor Lasers, Cavity

目　　錄

報告內容

I. Introduction

Although lots potential defect modes of different photonic crystal micro-cavity with ultra-low threshold, high Q-factor, and small mode volume have been reported in very recent years, most of these modes are not suitable for electrically driving. In this project period, our researches are focused on quasi-periodic photonic crystal micro-cavities, which are regarded as very potential devices for electrically driven due to its well-confined whispering-gallery-mode (WGM). However, in most general photonic crystal micro-cavities, WGM is hard to be sustained or with very low Q-factor due to the mismatch between the mode profile and the cavity geometry. One possible solution is using quasi-periodic photonic crystal (QPC). Under proper design, WGM can be well-confined in QPC micro-cavity. In addition, as the mirror of the micro-cavity laser, QPC shows much stronger confinement than that provided by photonic crystal. With high-Q WGM, an efficient QPC micro-cavity laser can be regarded as a better candidate for electrically driving than photonic crystal micro-cavity laser.

II. Design and Simulation

In this section, we report the characteristics of defect modes in different cavity designs in octagonal (8-fold) and dodecagonal (12-fold) quasi-periodic photonic crystals by using finite-difference time-domain (FDTD) method with effective index approximation.

At first, we investigate the octagonal (8-fold) QPC (OQPC) micro-cavity formed by 9 missing air holes. The cavity schematic is shown in Fig. 1 (a). The calculated defect mode profiles named K=0, K=1, K=2, and K=4 are shown in Fig. 1 (b), where K denotes the Block rotational number. They present WGM-like distribution. Although K=4 mode shows the zero field distribution at the central region, these modes are first- or second-order WGM and with low Q-factor and high threshold. In practice, these modes are not potential modes we discuss above.

Next, we then consider the micro-cavity formed by only one missing air-hole in the same OQPC lattice. The schematic of this single-defect OQPC micro-cavity is shown in Fig. 2 (a). The resonance modes are also calculated by FDTD method and the mode profiles with magnetic fields are shown in Fig. 2 (b). One can see that this cavity only supports two resonance modes, one is dipole mode and the other is quadrupole mode. In order to improve

the fusion with octagonal QPC micro-cavity and the micro-disk lasers, we design a new cavity geometry formed by single defect in octagonal QPCs as shown in Fig. 2 (a). The 8 nearest neighboring air holes are shifted outward to satisfy the constructive interference condition to form standing waves at the cavity edge. The calculated mode profile is shown in Fig. 2 (c). It shows a strong-confined WGM profile with azumital number four. This mode is sustained in the cavity not only by photonic band-gap (PBG) effect but also by total internal reflection (TIR) effect. In addition, it is worth to mention that the cavity size is 1.2μm, smaller than the diffraction limitation in micro-disk lasers.

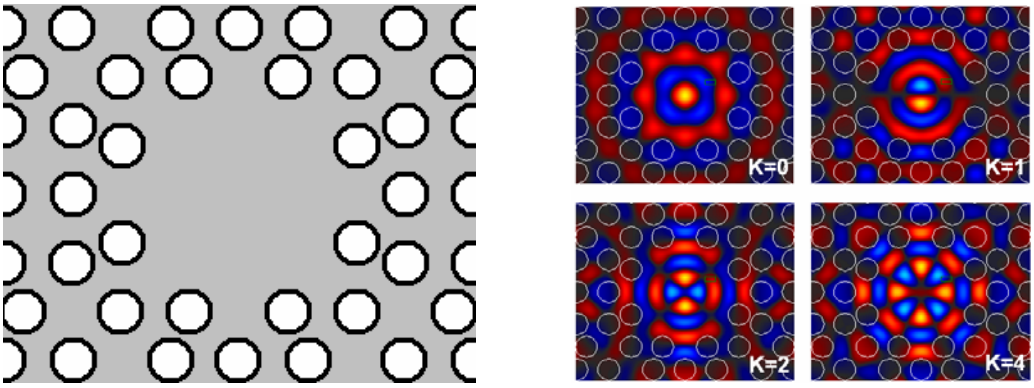

(a). (b).

Fig. 1 (a) Schematic of OQPC micro-cavity formed by 9 missing air holes. (b) Defect modes named K=0, K=1, K=2, and K=4.

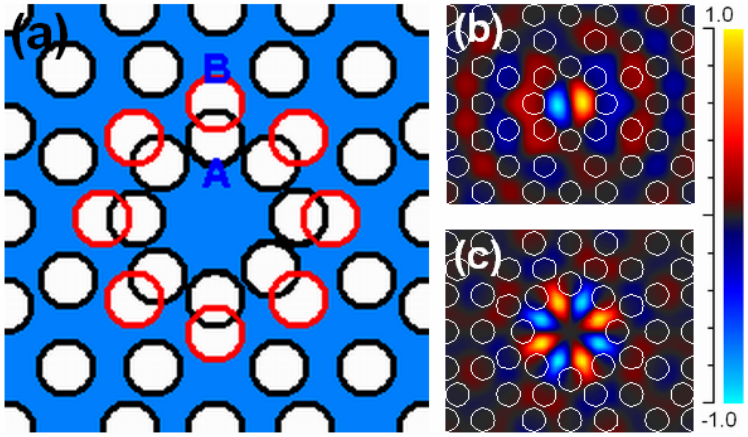

Fig. 2 (a) Schematic of original (position A) and modified (position B) OQPC single-defect micro-cavity. (b) Calculated dipole mode and (c) calculated WGM profiles of these two micro-cavities.

We also investigate the dodecagonal (12-fold) quasi-periodic photonic crystal (DQPC) micro-cavity formed by 7 missing air holes (D2) as shown in Fig. 1 (a). Comparing with OQPC, DQPC shows a more circular Brillioun zone, which implies the more efficient PBG

confinement effect. Besides, without any modification, the DQPC D2 micro-cavity can well sustain a high-Q WGM with azimuthal number six.

The calculated mode profile in magnetic field is shown in Fig. 3. It shows well-confined WGM with 12 lobes distributing along the cavity boundary. In fact, there is a very good fusion of quasi-periodic photonic crystal micro-cavity with conventional micro-disk lasers. This also could be a breakthrough for solving the problems of quality factor decreasing in minimized micro-disk lasers. Other resonance modes are also shown in Fig. 3.

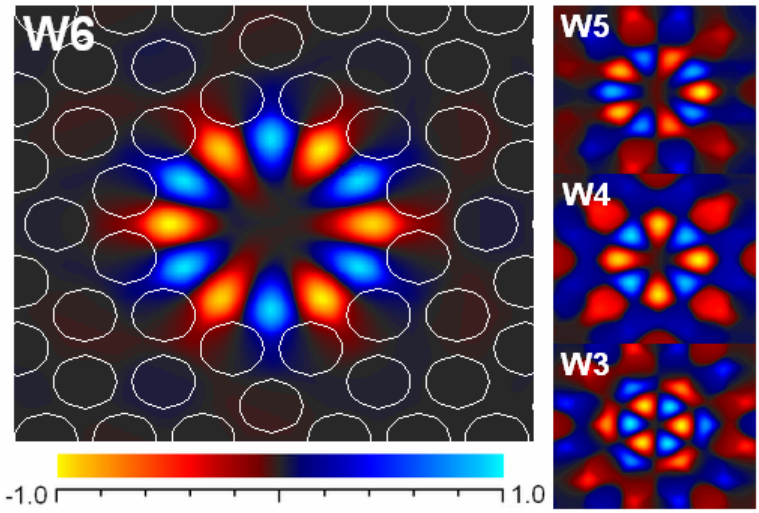

Fig. 3 Main resonance mode, WGM, with azumithal number six (W6 mode) is calculated by 2D FDTD method. The other two zero-order radial modes with azumithal number five (W5 mode) and four (W4 mode) and a first-order radial mode with azumithal number three (W3 mode) near the W6 mode in spectrum are also calculated.

III. Fabrication

Based on our well-developed fabrication process in photonic crystals, the designs mentioned above are well-fabricated. The epitaxial structure consisting of four 10 nm compressively-strained InGaAsP MQWs as the active layer with 1550 nm central wavelength under photoluminescence is prepared. First, the 140 nm silicon-nitride (SiN_x) layer served as hard mask for latter etching process is deposited on the epitaxial wafer by plasma-enhanced chemical vapor deposition (PECVD) system. And the polymerthylmethacrylate (PMMA) layer is spin-coated on the SiN_x layer. The QPC patterns are defined on the PMMA layer by electron-beam lithography and transferred to the SiN_x layer by reactive-ion etch (RIE) process with CHF_3/O_2 mixed gas. Then the patterns are

further transferred to MQWs by inductively-coupled plasma (ICP) dry-etching with $CH_4/Cl_2/H_2$ mixed gas at 150℃. At last, the membrane structure is formed by selective wet etching with the mixture of HCl and H_2O at 0℃. The top-view and side-view scanning electron microscope (SEM) pictures of different QPC micro-cavities designed in section II are shown in Fig. 4 (a)-(c).

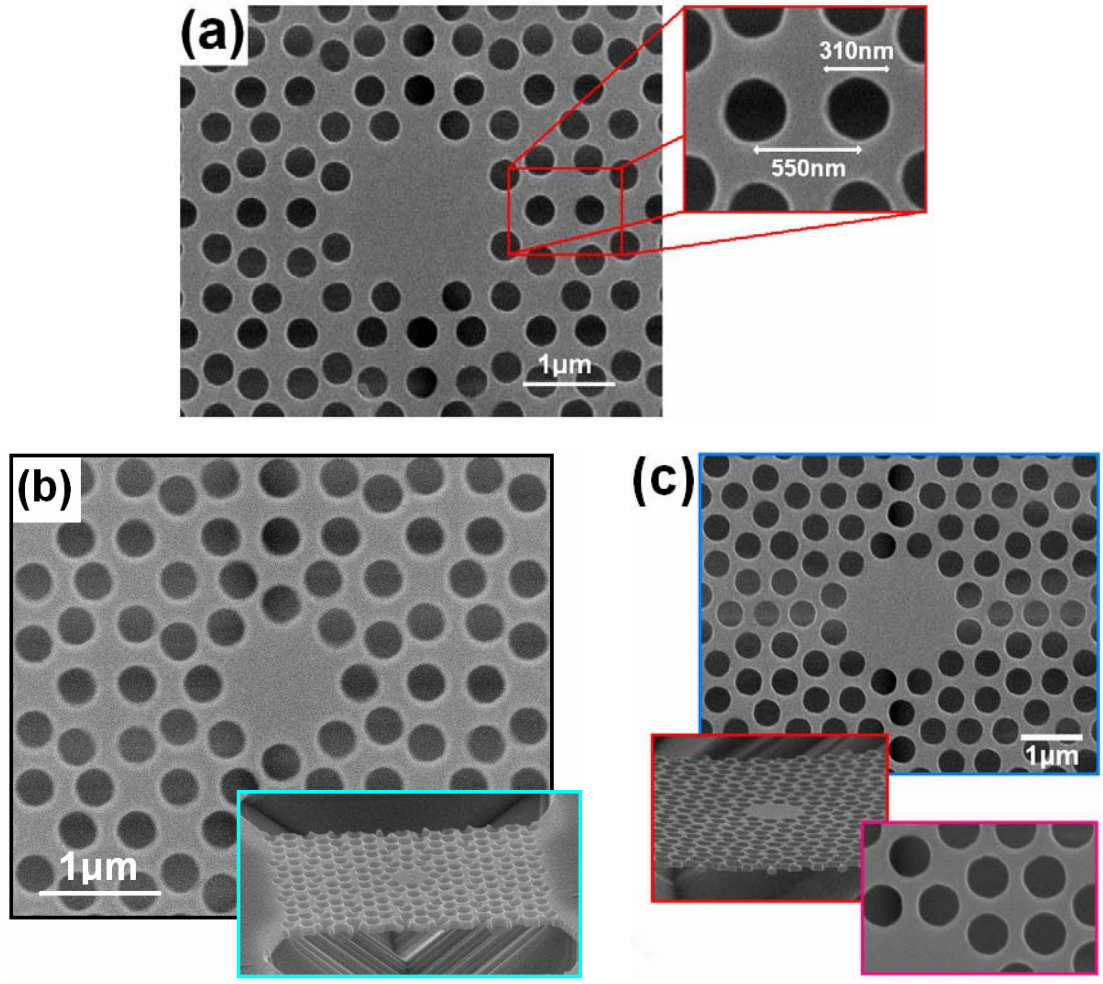

Fig. 4 Top-view and side-view SEM pictures of (a) OQPC D2 micro-cavity, (b) OQPC modified single-defect micro-cavity, and (c) DQPC D2 micro-cavity.

IV. Characterization & Discussion

In characterization, the micro-cavities are optically pumped by an 845 nm laser diode with focused pump spot size 1.5 μm in diameter. To avoid the thermal problems, the pump condition is set at 0.5% duty cycle with 200 KHz repetition rate. The emitted light is collected by a multi-mode fiber and its spectrum is detected by an optical spectrum analyzer (OSA) with 0.05 nm spectral resolution.

At first, we obtain the lasing action from OQPC D2 micro-cavity and recognize it as dipole mode (K=1). The light-in light-out curve (L-L curve) and typical lasing spectrum are shown in Fig. 5 (a) and (b). The threshold can be estimated as 0.7 mW and its full-width at half-maximum (FWHM) near threshold is 0.4 nm. We also obtain the relationship between intensity of the lasing mode versus angle. A specific polarization direction agrees with the mode distribution of the K=1 mode.

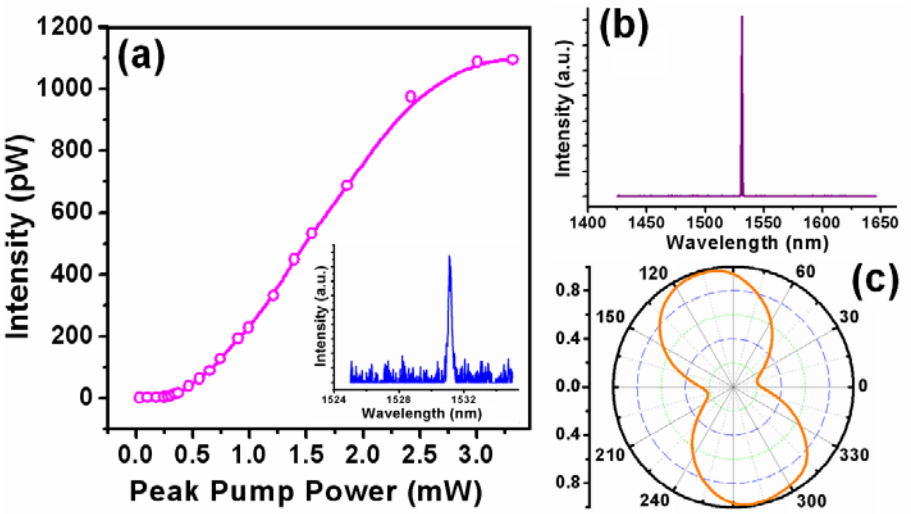

Fig. 5 (a) L-L curve of the K=1 mode. The spectrum near threshold is shown in the inset. (b) Lasing spectrum of the K=1 mode. (c) The relationship between intensity of the lasing mode versus angle.

In characterization of OQPC modified single-defect micro-cavity, the L-L curve and the typical lasing spectrum at room temperature are shown in Fig. 6 (a) and (b). The threshold can be estimated as low as 0.35 mW. The central lasing wavelength is 1499 nm with full-width at half-maximum (FWHM) 0.15 nm and 25dB SMSR. Its Q factor is about 7500, which is estimated from the measured line-width near the transparency pump power. The characteristics shown above all indicated the better performance than photonic crystal micro-cavity laser with similar cavity size.

Instinctively, one can add a central post or a central air-hole in the OQPC single-defect cavity region without disturbing the WGM. In addition, the side mode can be reduced or destroyed due to this extra central post or central air-hole. The top view SEM of fabricated cavity with a central air-hole is shown in the inset of Fig. 7. In measurement, the WGM is not affected significantly as predicted and the estimated Q factor is 6800, which is only a little smaller than that without a central air-hole. From the fabrication point of view, the larger central air-hole or central post implies larger fabrication tolerance and less sensitivity of the WGM to the central air-hole or central post. In addition, in the central post case, with

larger post size, there would be lower electrical resistance and faster thermal transition compared with smaller one. Thus, lower threshold voltage and better heat dissipation can be expected.

We also compare the lasing spectra with and without the central air-hole. We fabricate two devices with similar lattice parameters, one is with the central air-hole and the other is not. The measured lasing spectra in dB scale are shown in Fig. 7. One can see that the side mode is greatly reduced and the side-mode suppression-ratio (SMSR) increases from 25dB to larger than 30dB after adding a central air-hole. Besides, also shown in Fig. 7, the lasing mode is not affected significantly by the added central air-hole. We believe that similar results can be obtained for the central post case. This implies that this modified OQPC single-defect micro-cavity design is a promising structure for electrical injection with larger central post size tolerance.

In order to achieve the target of promising devices in ultra-dense integrated photonic circuit, we also fabricate modified OQPC single-defect micro-cavity arrays with different lattice periods from 8 to 3. The plot of lasing threshold versus number of cladding lattice periods is shown in Fig. 8. The threshold of OQPC micro-cavity with eight lattice periods is 0.71 mW and the lasing wavelength is 1454 nm. In Fig. 8, the thresholds are almost the same when the number of lattice periods is larger than six. Although the threshold increases when the number of lattice periods is smaller than six, the threshold with four lattice periods is 0.95 mW, which is only 36% increase compared to that with eight lattice periods. With four cladding lattice periods, the device size is only 3.5 μm × 3.5 μm as shown in the inset SEM picture of Fig. 8, which is a very condensed device size ever reported. Lasing action is not always observed when the number of lattice periods is reduced to three. We also fabricate triangular lattice PC micro-cavity with similar cavity size formed by seven missing air holes (D2 cavity) for comparison. As shown in Fig. 8, the thresholds of triangular lattice PC D2 micro-cavities with eight, six, and four cladding lattice periods are 0.65 mW, 0.9 mW, and 1.48 mW, respectively. And the lasing wavelength is near 1560 nm, which aligns better with the gain peak of MQWs, leading to a smaller threshold of triangular lattice PC D2 micro-cavity with eight lattice periods than that of OQPC micro-cavity. For the number of lattice periods below seven, one can see that the thresholds of OQPC micro-cavities are much lower than that of triangular lattice PC D2 micro-cavity even the lasing wavelength of the former is much farther away from the gain peak of MQWs. In addition, the threshold of triangular lattice PC D2 micro-cavity increases about 130% from eight periods to four periods, which is much larger than the 36% of OQPC micro-cavities.

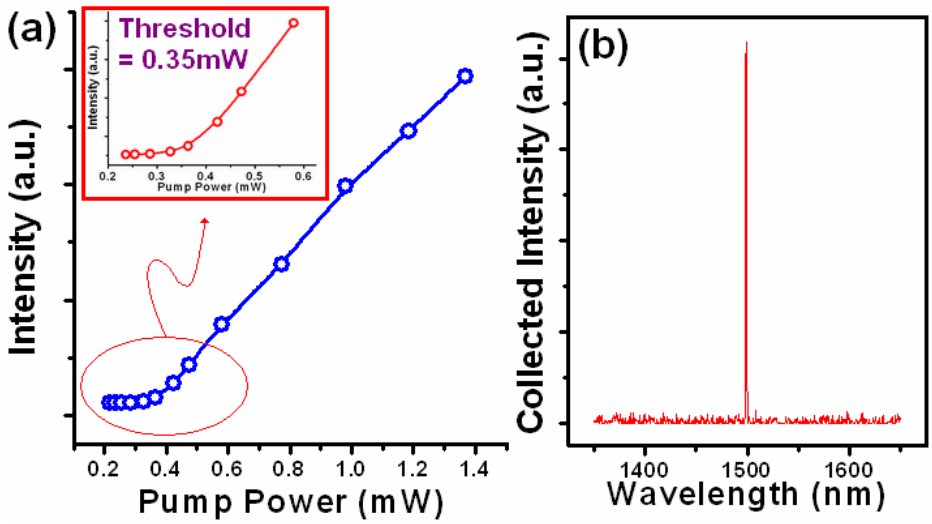

Fig. 6 (a) L-L curve. The inset shows the L-L curve near threshold and indicates its threshold as low as 0.35 mW. (b) Lasing spectrum at 1499 nm with 0.15 nm FWHM.

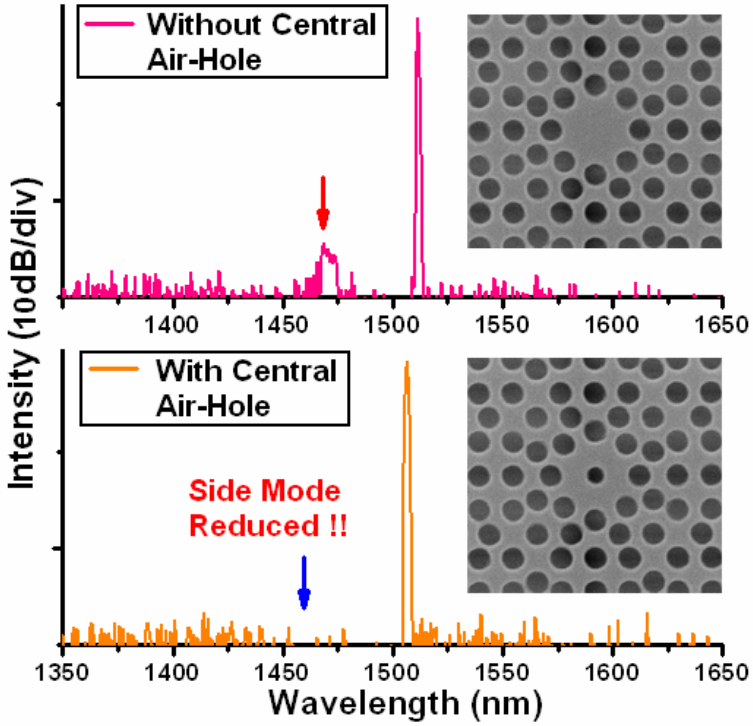

Fig. 7 Lasing spectra in dB scale without (top) and with (bottom) a central air-hole. The side mode is greatly reduced by inserting the central air-hole.

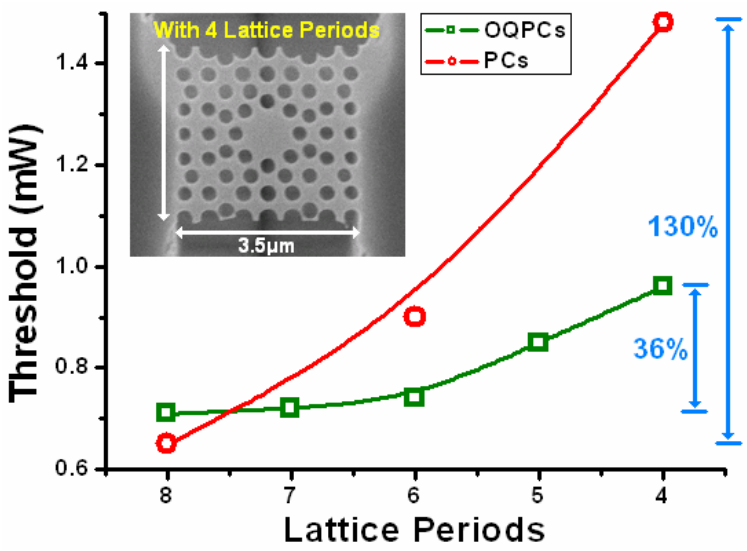

Fig. 8 Plot of lasing threshold versus number of cladding lattice periods. There is only 36% increase in threshold of OQPC micro-cavity when the number of lattice periods is reduced from eight to four, which is much smaller than the 130% of triangular lattice photonic crystal D2 micro-cavity. The inset shows the SEM image of the OQPC micro-cavity with four lattice periods and very condensed size of 3.5 μm × 3.5 μm.

In the photoluminescence (PL) measurements of DQPC D2 micro-cavity laser, the micro-cavity is optically pulse-pumped at room temperature by the same pump condition. The L-L curve and typical lasing spectrum of DQPC D2 micro-cavity are shown in Fig. 9 (a) and (b).We obtain the ultra-low threshold 0.15 mW of DQPC D2 micro-cavity from the L-L curve and its FWHM is 0.15 nm at 1572 nm lasing wavelength. We also fabricate PC D2 micro-cavity laser with triangular lattice by the same process and on the same wafer for comparisons. Its L-L curve and SEM picture are shown in Fig. 9 (a) and its inset. The threshold of PC D2 micro-cavity laser with single-mode lasing is 0.6 mW and its FWHM is around 0.3 nm at a similar lasing wavelength, which both indicate the better performance of DQPC lasers resulted from the more uniform and efficient confinement provided by the high symmetric Brillouin zone of quasi-lattice and the presence of WGM. Besides, the threshold of DQPC D2 micro-cavity laser is also lower than the 0.3 mW of modified single-defect micro-cavity laser with lower symmetry OQPCs.

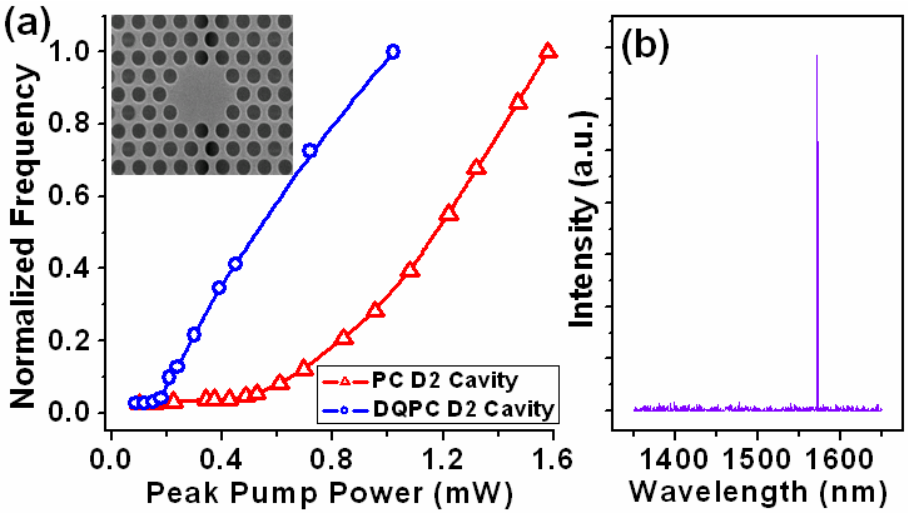

Fig. 9 Typical L-L curves of DQPC and triangular PC D2 micro-cavity lasers. (b) Typical lasing spectrum of DQPC D2 micro-cavity laser.

In Fig. 3, the W6 mode profile has good consistency with the gears formed by the 12 nearest air-holes surrounding the cavity. This also implies the strong mode dependence of W6 mode on the positions of 12 nearest air-holes. To obtain more direct evidence supporting this assumption, we randomly vary the positions of the 12 nearest air-holes (denoted by red circles, region-A) and the outer air-holes (denoted by blue circles, region-B) separately, as shown in Fig. 10 (a). The degrees of variation are 1%, 2%, 3%, 4%, 5%, and 7% of lattice constant with fixed r/a ratio and lattice constant. Lasing spectra of devices with randomly varying the air-hole positions in region-A and region-B are shown in Fig. 10 (b). The wavelength fluctuations for the region-A and B cases are 19 nm and 2.5 nm, respectively. In the region-A case, when 12 nearest air-holes are randomly shifted, the original W6 mode tends to self-optimize its resonance behavior according to the position fluctuation. During this optimization process, the constructive interference condition provided by the nearest air-holes is degraded. However, in the region-B case, it can be treated as the modal boundary condition (positions of 12 nearest air-holes) is invariant, leads to almost the same lasing wavelength and threshold. The small wavelength variation 2.5 nm in the region-B case is caused by very slight hole-radius differences occurred during the electron-beam lithography process. In Fig. 10 (a), we also show examples of mode distortions for the two cases with the same variation degree 5%. One can see significant mode distortion for the region-A case, but not for the region-B case compared to Fig. 3. As a result, the lasing wavelength variation is mainly caused by randomly varying the region-A lattice, which indicates the strong mode dependency of W6 mode on the 12 nearest air-holes.

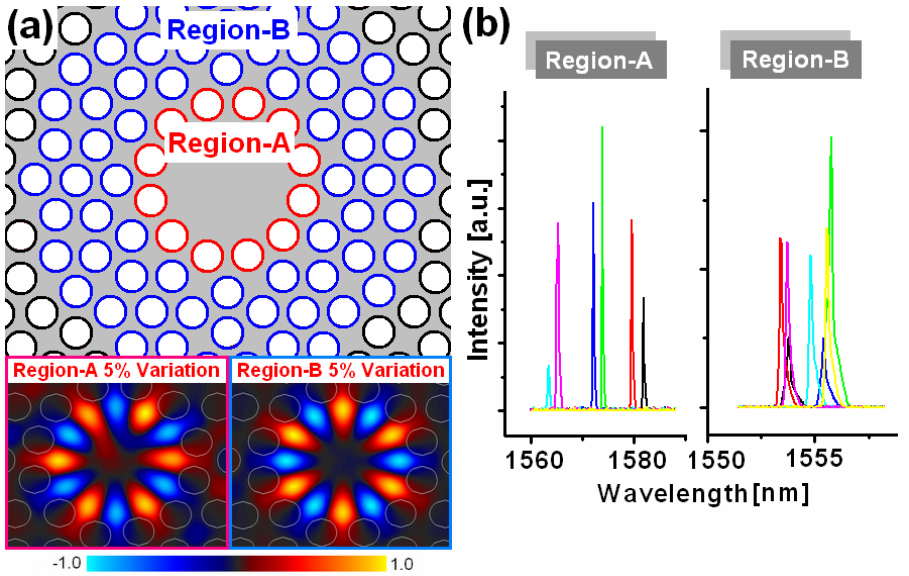

Fig. 10 (a) Illustration of two variation regions, the 12 nearest air-holes (denoted by red circles, region-A) and the outer air-holes (denoted by blue circles, region-B) in DQPC D2 micro-cavity. The mode distortions of these two cases with the same variation degree 5% are also shown. (b) Lasing spectra of devices with different variation degrees in region-A and region-B. Lasing wavelength variations for the region-A and region-B cases are 19 nm and 2.5 nm, which show strong mode dependence on the 12 nearest air-holes.

V. Publications

(I) Journals

1. **P. T. Lee**, T. W. Lu, F. M. Tsai, and T. C. Lu, "Investigation on Whispering Gallery Mode Dependence on Cavity Geometry of Quasi-Periodic Photonic Crystal," *Appl. Phys. Lett.* (2006) (Accepted for Publication)
2. **P. T. Lee**, T. W. Lu, F. M. Tsai, T. C. Lu, and H. C. Kuo, "Whispering-Gallery-Mode of Modified Octagonal Quasi-Periodic Photonic Crystal Single-Defect Micro-Cavity and its Side-Mode Reduction," *Appl. Phys. Lett.* **88**, 201104 (2006)
3. W. Kuang, J. R. Cao, T. Yang, S. J. Choi, **P. T. Lee**, J. D. O'Brien, and P. D. Dapkus, "Classification of modes in suspended membrane, 19 missing holes photonic crystal micro-cavities," *J. Opt. Soc. Am. B,* **22**, pp.1092-1099 (2005)
4. J. R. Cao, W. Kuang, S. J. Choi, **P. T. Lee**, J. D. O'Brien, and P. D. Dapkus, "Threshold dependence on the spectral alignment between the quantum-well gain peak and the cavity resonance in InGaAsP photonic crystal lasers," *Appl. Phys. Lett.* **83**, 4107 (2003).

(II) Conferences

1. F. M. Tsai, **P. T. Lee**, T. W. Lu, and T. C. Lu, “Fabrication and Characteristics of Two-Dimensional Quasi-Periodic Photonic Crystal Lasers,” CMKK6, CLEO/QELS’06 (2006)
2. T. W. Lu, F. M Tsai, **P. T. Lee**, and T. C. Lu, “Modified Octagonal Quasi-Periodic Photonic Crystal Single-Defect Micro-Cavity Lasers,” JWB11, CLEO/QELS’06 (2006)
3. **P. T. Lee**, T. W. Lu, F. M. Tsai, and T. C. Lu, “Lasing Action of Octagonal Quasi-Periodic Photonic Crystal Micro-Cavities,” IEEE/LEOS IPRM’06 (2006)
4. T.-W. Lu and **P. T. Lee**, "Thermal Characteristics of Two-Dimensional Photonic Crystal Lasers," *IEEE WOCN'05*, 1064, Dubai, UAE (2005)
5. K. H. Ten, H. W. Zan, C. P. Ko, P. K. Liu, T. Y. Chang, K. H. Su, C. S. Wei, **P. T. Lee**, Ch. H. Chen, C. M. Yeh, and Jennchang Hwang, “Organic thin-film transistors with AlN film as a gate-insulator by RF/ICP Sputtering,” EuroDisplay 2005 Oral Presentation.
6. **P. T. Lee**, H. W. Zan, S. C. Wei, C. C. Lee, J. C. Ho, and T. H. Hu, “Thermal Behavior and Self-Heating Effect in Pentacene-Based Thin Film Transistors,” International Display and Manufacturing Conference (IDMC), Wed-12-05, Taiwan (2005).
7. F. M. Tasi, **P. T. Lee**, and T. C. Lu, “Fabrication and characterization of two-dimensional quasi-periodic photonic crystal lasers,” *OPT’05*, A-FR-I-1-1, Taiwan (2005)
8. H. C. Kuo, Y. H. Chang, F. I. Lai, **P. T. Lee**, and S. C. Wang, “High performance 1.27 μm InGaAs:Sb-GaAsP quantum wells vertical cavity surface emitting laser,” IEEE 19th International Semiconductor Laser Conference, pp. 97- 98, Sept. 2004.
9. T. W. Lu and **P. T. Lee**, "Thermal Characteristics of Two-Dimensional Photonic Crystal Lasers," *OPT’04*, B-SA-VII-1-6, Taiwan (2004)
10. Y. H. Chang, H. C. Kuo, F. I. Lai, Y. A. Chang, **P. T. Lee**, and S. C. Wang, “Fabrication of high speed single mode 1.27 μm InGaAs:Sb-GaAsP quantum wells vertical cavity surface emitting laser,” International Conference on Solid State Devices and Materials (SSDM), Tokyo, Japan 2004.

計畫成果自評

During the past year, we have accomplished many things and demonstrated the ability to obtain high quality results for photonic crystal lasers. We have published a paper on modified octagonal quasi-periodic photonic crystal single-defect micro-cavity laser on Applied Physics Letters, and a paper investigating properties of whispering gallery modes of quasi-periodic photonic crystals is accepted for publication on Applied Physics Letters. Another paper submitted to Photonics Technology Letters about fabrication tolerance of quasi-periodic photonic crystal lasers is under minor revision. We also presented our results on various international conferences. We are very glad that our research results have been recognized by high impact factor journals and top conferences. These results show that we have found a cavity structure that is suitable for current ejection and we are the first group to propose this kind of structure for photonic crystal-based laser cavities. We hope that we can continue this work and obtain more exciting and important results in the near future.